WAFER LEVEL VACUUM PACKAGED DE-COUPLED VERTICAL GYROSCOPE BY A NEW FABRICATION PROCESS

H. Song, Y.S. OH, I.S. Song, S.J. Kang, S.O. Choi , H.C. Kim, B.J Ha, S.S. Baek, C.M.Song
Microsystems Lab. S&C sector,
Samsung Advanced Institute of Technology,
P.O BOX 111, Suwon 440-600, Korea,
Tel: (82)-331-280-9281, Fax: (82)-331-280-6955, e-mail: hsong@saitgw.sait.samsung.co.kr

ABSTRACT

The high reliable, wafer level vacuum packaged and de-coupled vertical microgyroscope was developed. The de-coupled gyroscope that had four driving springs and two sensing springs was designed and fabricated. And the new fabrication process that could make a high aspect ratio and use a thick single crystalline silicon as a structure layer was proposed. The vacuum environment for operating a vibratory gyroscope was accomplished with vacuum packaging in wafer level. The vacuum level of ambient pressure was about 150mTorr. The resolution of the gyroscope was 0.013 °/sec/Hz$^{1/2}$. The output nonlinearity was below 2% in ±100 °/sec full scale.

INTRODUCTION

Recently, there is increasing needs of the micro gyroscope in the commercial application filed, such as the automobile, the camcorder, the VR HMD set (Virtual reality head mount display), and so on. However, though the many researchers have tried to develop the reliable and low-cost gyroscope, it is not commercially available yet. Until now, there are still some problems, such as the exact tuning, the wafer level vacuum packaging, and the temperature dependency on the structure material. [1-4]

The lateral gyroscope can be fabricated easily with one mask process. [5-6] In the contrary, there are a lot of activities for commercialization of the vertical gyroscope that measures in-plane angular velocity, because it needs more complex fabrication process such as the surface micromaching. [7-10]

In the resonant vibratory gyroscope, when the driving and the sensing frequencies are exactly tuned, the sensitivity is maximized. However, the driving and the sensing frequencies of the fabricated gyroscope are barely same due to fabrication error, even though the gyroscope has the exactly same frequencies in design stage. To close two mode frequencies of the gyroscope, the electrostatic tuning is needed. On the other hand, the coupled gyroscope that used same spring in driving and sensing modes shows mode coupling effect when the difference between driving and sensing mode frequencies is smaller than 100 Hz.[11] Therefore, the de-coupled structure design is required.

The surface micromachinig using LPCVD poly-silicon is one of the most convenient process as for MEMS (micro electro-mechanical system). However, the LPCVD poly-silicon layer easily gets residual stress and stress gradient that make MEMS structure unstable. Furthermore, for the de-coupling design, the thick structure is needed, but it's hard to fabricate over 10μm-thick LPCVD poly-silicon structure.[12]

In this paper, we present the new vertical de-coupled gyroscope which is fabricated by the new mixed micromachining technology to have a high aspect ratio of single crystalline silicon structure and the vacuum packaging method in wafer level.

PRINCIPLES AND DESIGN

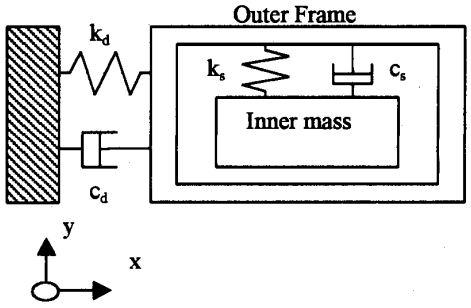

Fig. 1 The Schematic of De-coupled the gyroscope

Figure 1 shows the schematic of a vibratory de-coupled gyroscope. A vibratory de-coupled gyroscope is based on a pair of driving and sensing resonators. In the vibratory gyroscope, to increase the sensitivity, the driving and the sensing frequencies should be exactly tuned. However, the coupled gyroscope structure to have the same spring for the driving and sensing modes shows mode coupling effect that is caused by the mechanical interference between the driving and the sensing modes, when the driving and sensing frequencies become closer. To eliminate the coupling effect, the gyroscope should have unconstrained spring for the driving and the sensing mode.

0-7803-5273-4/00/$10.00 ©2000 IEEE

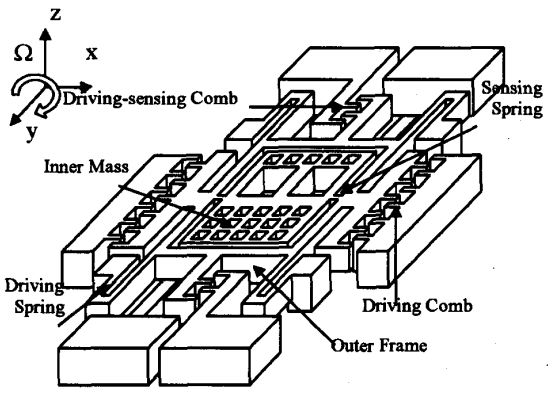

Fig. 2 The schematic of the new gyroscope

The schematic of the de-coupled vertical gyroscope is shown in Fig.2. The gyroscope has 4-driving springs suspending the whole mass, the driving comb electrodes, and the driving-sensing comb electrodes. Under the inner mass, there are the bottom electrodes that sense the tilting of inner mass. The outer frame is connected to the substrate by 4-driving springs. The mass devides into two parts, that is to say, the inner mass and the outer frame. The inner mass and the outer frame that is around the inner mass are connected with two torsional sensing springs. When the driving voltage applies on the driving comb electrode on the side of the outer frame, the mass oscillates along x-axis with the driving frequency. The gyroscope rotates about y-axis, which generates Coriolis force along the z-axis. The generated Coriolis force makes the asymmetry inner mass tilt, which makes the capacitance between the inner mass and the bottom electrode change.

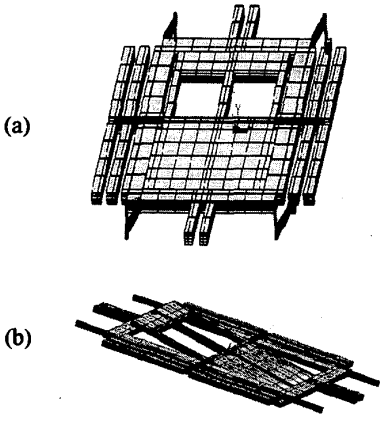

Fig. 3 ANSYS 5.3 ® FEM Modal Simulation Result; (a) Driving Mode (2.97 kHz), (b) Sensing Mode (3.13 kHz)

For a design of the gyroscope, FEM modal simulation is used for predicting the frequencies and the deformed shapes of the driving and sensing modes. Figure 3 shows the result of ANSYS FEM simulation. The frequencies of the driving (Fig. 2a) and the sensing mode (Fig 2b) are 2.97kHz and 3.13kHz, respectively. The sensing frequency is designed about 100Hz higher than the driving frequency because of the electrostatic tuning and the fabrication tolerance. And, the result of simulation conforms that there is no interference between driving and sensing mode, because of unconstrained spring structure.

FABRICATION PROCESS

In general, to fabricate the vertical gyroscope that has the bottom electrode, the surface micromachining using LPCVD poly silicon is used. However, the poly crystalline silicon structure is made to be unstable due to the residual stress and the stress gradient. Besides, it is difficult for LPCVD poly silicon to be deposited with over 10μm-thick because of the repeatability. In the new mixed micromachining, the single crystalline silicon structure with a high aspect ratio can be fabricated without residual stress or stress gradient. Furthermore, it can fabricate the structure as various as the surface micromachining.

Figure 4 shows the mixed micromachining fabrication process. At first, a highly doped n-type wafer (0.01 ~ 0.05 Ω·Cm) was prepared for the structure layer. On the structure wafer, TEOS was deposited for the sacrificial layer, and then the anchor pattern was formed. The LPCVD poly silicon layer was deposited and formed for the bottom electrode and the feedthrough for the interconnection. On the LPCVD poly silicon layer, Si_3N_4, SiO_2 and the 10μm-thick epitaxy poly silicon layers were passivated for the insulation and the substrate wafer bonding. The epitaxy poly crystalline silicon layer was polished for SDB (Silicon Direct Bonding). After the substrate wafer was bonded on the polished epi layer to handle, the structure layer was lapped and polished to 40μm thickness with CMP (Chemical Mechanical Polishing). For the electric pad, Cr/Au was deposited and patterned. The gyroscope structure was formed with deep etcher, ICP RIE. Finally, the sacrificial layer was removed by BOE (Buffered Oxide Etcher) solution to release the gyroscope structure.

To improve the performance of the vibratory gyroscope, the gyroscope needs vacuum environment to operate in. To make vacuum environment, we used the wafer level vacuum packaging process. The "cap wafer" to encapsulate the sensor structure, was fabricated with TMAH anisotropy wet etching. A 300μm-thick wafer

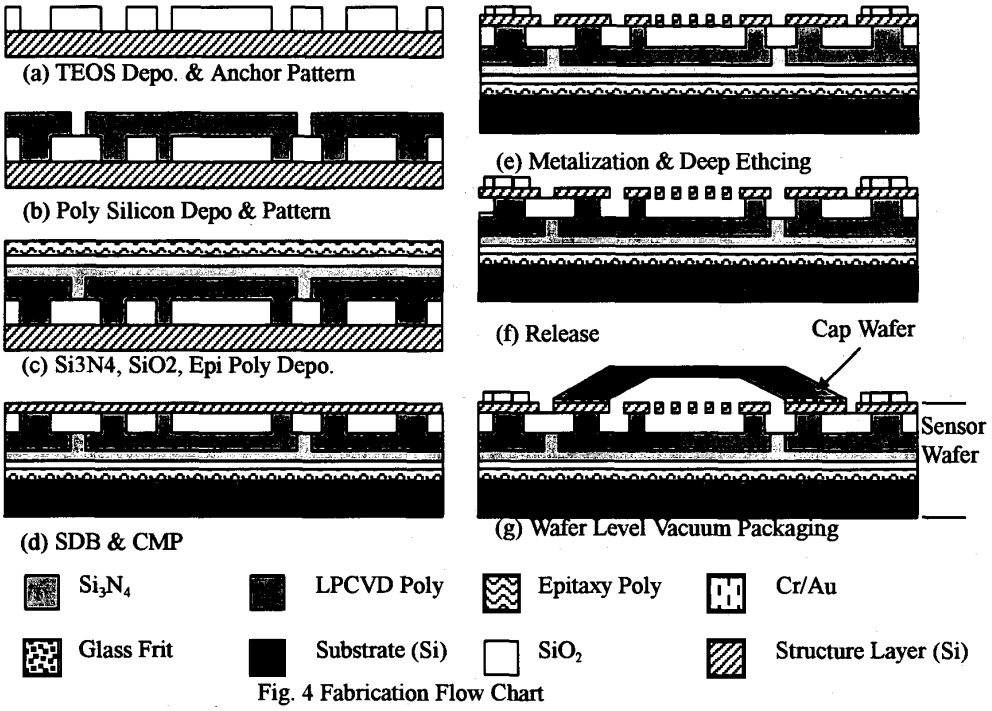

Fig. 4 Fabrication Flow Chart

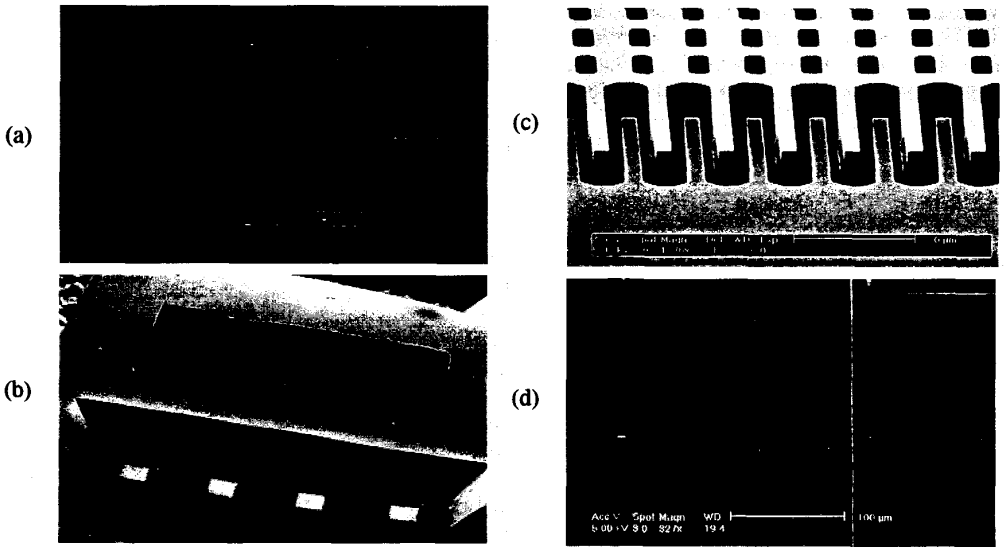

Fig. 5 The fabricated de-coupled vertical gyroscope, (a) the perspective view, (b) the wafer level vacuum packaged gyroscope, (c) the closed view of comb electrode, and (d) the pad and interconnection feedthrough.

having SiO_2 layer was patterned for electric pad opening, and then etched about 40μm as same as the thickness of the ceil of cavity. On the other side of the wafer the cavity pattern was formed for the moving part. And, the etching process continues until the pattern for electric pad opening was formed via hole. Before the glass frit was patterned, the SiO_2 masking layer was removed, and then the new SiO_2 layer was passivated for insulation. The fabricated cap wafer was aligned to the sensor structure in wafer level. In the vacuum chamber, the wafer was heated to 450°C until the glass frit melts completely. The wafer bonded by glass frit was cooled

to room temperature. The packaged sensor in wafer level was diced and mounted to the sensing circuit for the test.

Figure 5a is the SEM image of the fabricated sensor. The fabricated gyroscope structure is shown through the broken ceil of the package in fig. 5b. Figure 5c shows a closed view of the driving comb electrode. The inter-comb distance was 1.5μm. Figure 5d is the SEM image of the interconnection feedthrough under the structure layer.

CIRCUIT AND RESULT

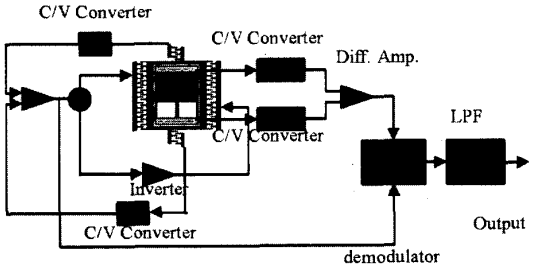

Fig.6 The schematic of the detection circuit

The schematic diagram of the detection circuit is shown in Fig. 6. The driving-sensing comb electrode detects the position of the mass along the driving direction. The detected signal is amplified and fed back to the driving comb electrode. The feed back loop makes the mass oscillating itself at driving mode frequency even if frequency varies by the environment and/or it has a displacement-force nonlinear behavior. An applied angular velocity generates Coriolis force, which changes the capacitance between the inner mass and the bottom electrode. The capacitance variance is transformed to the voltage signal by the C/V converter. After the signal is amplified differentially, the signal is demodulated to remove the carrier signal. Finally, the signal is filtered to reduce the high frequency noise with a low pass filter (LPF).

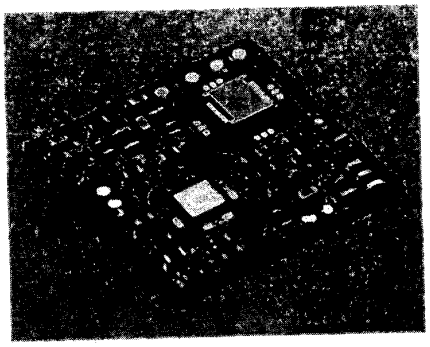

Fig. 7 The packaged gyroscope mounted on PCB with ASIC.

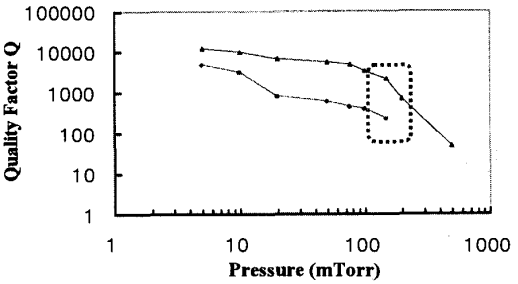

Fig. 8 Q-factor vs. Vacuum Level; the triangle mar is for driving mode Q-factor, the circle is for driving mode Q-factor and deshed box is the Q-factor of wafer level vacuum packaged gyroscope.

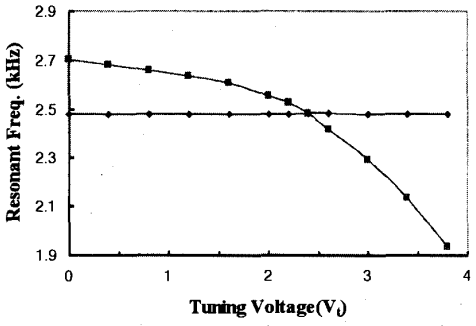

Fig.9 The frequency change by Tunning Voltage; the diamond markis driving mode frequency and the square is sensing mode f

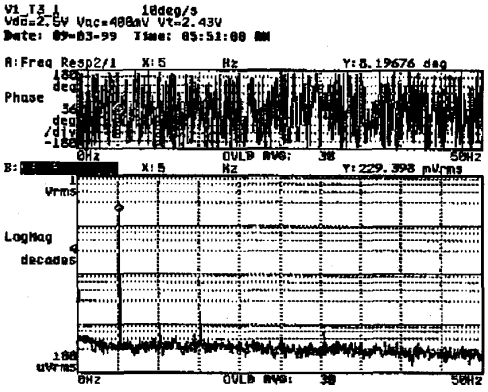

Fig. 10 The rate output spectrum of gyroscope; the input rate is 5Hz-10 °/sec pk-to-pk.

Figure 7 is a photograph of the gyroscope mounted on PCB for performance test. The wafer level vacuum packaged gyroscope and detection circuit ASIC were mounted on the rate table as a reference rate input instrument.

Figure 8 shows the mechanical Q factor of the driving and the sensing mode as a function of the ambient

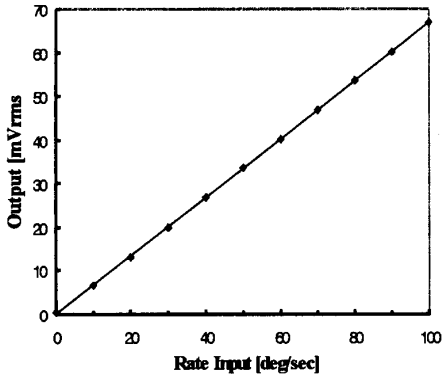

Fig. 11 The rate input vs. the output

pressure from 1 mTorr to 1 Torr. From this result, the Q factor was affected significantly by an ambient pressure, and the sensing mode was strongly damped by air. At 150 mTorr, the Q factor of the driving and sensing modes was mesured to about 2000 and 500, respectively. The Q-factor of wafer level vacuum packaged gyroscope for driving mode was measured to about 2000. Therefore, the ambient pressure for the packaged gyroscope was estimated at 150 mTorr.

The mismatching of the driving and sensing frequencies by fabrication tolerance and/or other reason resulted in low sensitivity. However, the driving and sensing frequencies could be made to approach each other by changing the effective stiffness of the sensing spring by using a dc-bias voltage (V_t) on the sensing electrode. As shown in the Fig. 9, the sensing frequency was decreased to lower frequency by increasing the tuning voltage (V_t). On the other hand, the driving frequency was kept constant irrespective of the tuning voltage.

Figure 10 show the rate output spectrum of the gyroscope when the 5Hz-10 °/sec peak-to-peak rate input is applied. By comparing the 5Hz output spectrum and the noise floor, the noise equivalent resolvable rate was about 0.013 °/sec/$Hz^{1/2}$. Figure 11 shows the rate output of the gyroscope as a function of the input rate from 0 to 100 °/sec. The output nonlinearity was below 2% in ±100 °/sec full scale.

CONCLUSION

We developed the de-coupled vertical gyroscope measuring out-of-plane angular velocity. To reduce coupling effect, the de-coupled gyroscope had unconstrained springs for the driving and the sensing modes. And the gyroscope was fabricated with the new mixed micromachining having the 40μm-thick single crystalline silicon structure without residual stress or stress gradient. The fabricated gyroscope was vacuum packaged in wafer level with the interconnection feedthrough under the structure layer. The vacuum level of ambient pressure was about 150mTorr. The noise equivalent rate of the gyroscope was 0.013 °/sec. The output nonlinearity was below 2% in ±100 °/sec full scale.

The gyroscope could be used for a hand wobble sensor for camcorders, or a 3-dimansional mouse, and in the future it is expected to be applied to the yaw rate and an acceleration sensor for a vehicle dynamic control or a navigation system.

Reference

[1] M. Lutz, W. Golderer, J. Gerstenmeier, et al. , "A Precision Yaw Rate Sensor in Silicon Micromachining", 1997 International Conference on Solid-State Sensors and Acturator , Chicago, IL, Jun.16-19, p. 847-850, 1997.

[2] D. R. Sparks, S. R. Zarabadi, et al, "A CMOS Integrated Surface Micromachined Angular Rate Sensor; It's Automotive Applications", 1997 International Conference on Solid-State Sensors and Acturator , Chicago, IL, Jun.16-19, p. 851-854, 1997.

[3] J. A. Geen, "A Path to Low Cost Gyroscopy", Solid-State Sensor and Acturator Workshop, Hilton Head, South California, June 8-11, p. 51~54, 1998.

[4] C.M. Song, M.N. Shin, "Commercial Vision of Silicon-based Inertia Sensors", Sensors and Acturator A 66, 1998, p. 231.

[5] K.Y Park, H. S Jeong, et al, "Lateral Gyroscope Suspended by Two Gimbals through High Aspect Ratio Etching", Transducer '99, FL, USA, p. 612-617, 1999.

[6] S.S. Baek, Y.S. Oh, B.J. Ha, et al, "A Symmetrical Z-Axis Gyroscope with A High Aspect Ratio Using, Simple And New Process", MEMS '99 Conference Proceeding, p.612, 1999.

[7] S. D An, Y. S Oh, et al, "Dual-Axis gyroscope with Close-loop Detection", in Proc. IEEE MEMS Workshop, Heidelberg, Germany, p. 328~333, 1998.

[8] Y. S Oh, B. L Lee, et al, "A Surface Micromachined tunable vibratory gyroscope", MEMS '97, Nagoya, Japan, p. 272-277, 1997

[9] T. Fujita, K. Hatano, et al, "Vacuum sealed Silicon Bulk Micromachined Gyroscope", Trensducers'99, p. 914~917, 1999

[10] Scott Adams, James Groves, et al, "A Single-Crystal Silicon Gyroscope with Decoupled Drive and Sense", The SPIE Conference on Micromachined Devices and Components V, p. 74~83, Sep. 1999

[11] B.L Lee, Y.S. Oh, et al , "A Dynamically Tuned Vibratory Micromichanical Gyroscope and Accelerometer", SPIE 1997, Dec.

[12] Y. B. Ganchandain, M.N. Shin, Impact of Long, "High Temperature Anneals on Residual Stress in Polysilicon", Transducer'97 Proceeding , 1997, Jun